Histochem Cell Biol (2008) 130:795–805
DOI 10.1007/s00418-008-0507-7

REVIEW

Fluorescence fluctuations analysis in nanoapertures: physical concepts and biological applications

Pierre-François Lenne · Hervé Rigneault · Didier Marguet · Jérôme Wenger

Accepted: 2 September 2008 / Published online: 18 September 2008

Abstract During the past years, nanophotonics has provided new approaches to study the biological processes below the optical diffraction limit. How single molecules diffuse, bind and assemble can be studied now at the nanometric level, not only in solutions but also in complex and crowded environments such as in live cells. In this context fluorescence fluctuations spectroscopy is a unique tool since it has proven to be easy to use in combination with nanostructures, which are able to confine light in nanometric volumes. We review here recent advances in fluorescence fluctuations' analysis below the optical diffraction limit with a special focus on nanoapertures milled in metallic films. We discuss applications in the field of single-molecule detection, DNA sequencing and membrane organization, and underscore some potential perspectives of this new emerging technology.

Keywords Biophotonics · Single molecules · Fluorescence fluctuations · Nanostructures · Plasma membrane

P.-F. Lenne (✉) · H. Rigneault · J. Wenger (✉)
Institut Fresnel, UMR 6133 CNRS,
Aix-Marseille University and Ecole Centrale Marseille,
Domaine Universitaire de Saint Jérôme,
13397 Marseille Cedex 20, France
e-mail: lenne@fresnel.fr

J. Wenger (✉)
e-mail: jerome.wenger@fresnel.fr

D. Marguet
Centre d'Immunologie de Marseille-Luminy,
Université de la Méditerranée, Parc scientifique de Luminy,
Case 906, 13288 Marseille Cedex 09, France

D. Marguet
Institut National de la Santé et de la Recherche Médicale,
UMR 631, Parc scientifique de Luminy, Case 906,
13288 Marseille Cedex 09, France

D. Marguet
Centre National de la Recherche Scientifique,
UMR 6102, Parc scientifique de Luminy, Case 906,
13288 Marseille Cedex 09, France

Introduction

Watching a fluorescent single molecule in an empty space or in a crowd does not require the same performances. To be detected the signal of a single molecule must first overcome the background. The second requirement is the ability to resolve individual objects. While such conditions can now be adequately fulfilled for a single molecule in an empty space, their achievement is challenging in a crowded environment. Different strategies have been proposed to tackle these issues. A very elegant way consists in changing a crowd in a quasi-empty space by switching on only a small number of molecules, which can be resolved: this is the key of photo-activation localization microscopy (Betzig et al. 2006) or stochastic optical reconstruction microscopy (Rust et al. 2006). These two methods have the ability to generate ultra-resolved images by photo-switching, in successive rounds, small fractions of photo-activable (or photo-convertible) fluorophores attached to the molecule under study. Alternatively, it is possible to sharpen the observation volume by shaping the light excitation/emission active volume. To do so Stimulated Emission Depletion Microscopy (Klar and Hell 1999) uses non-linear optical effects to deplete fluorescence of molecules everywhere in a confocal volume except in its central region as small as a sphere of 40- to 45-nm diameter (Schmidt et al. 2008). Finally, using nanostructures light can be confined

in volumes at least three orders of magnitude smaller as compared to confocal microscopy (Levene et al. 2003). Here we review recent literature on dynamic measurements using nanostructures with a special emphasis on nanoapertures milled in metallic films. As will be discussed below, nanoapertures provide small observation volumes but also, in some conditions, enhanced fluorescence detection.

We will first present what photonic structures are by introducing simple optical concepts, which explain their properties. Then we will show how their use extends the applicability of dynamic measurements performed by fluorescence correlation spectroscopy. Such experimental combination provides an original approach to tackle issues in a variety of fields, amongst which we will review findings on enzyme kinetics, DNA sequencing and dynamic membrane organization. We will also present possible ways for instrument developments and discuss unexplored questions that such methods may unravel.

Physical concepts

Nanophotonic structures

A photonic structure is defined as a structure, which is able to affect the propagation of light. In this respect, a single lens can be viewed as a photonic structure as it has the capability to concentrate the optical energy at its focus. A nanophotonic structure is simply a photonic structure with spatial scales ranging from few nanometers to few hundreds of nanometers. This latter scale is comparable to the wavelength of visible light and is associated with the so-called diffraction regime. In this regime, the light-matter interaction is maximal and usually highly wavelength dependent. This is nicely illustrated in diffraction gratings, which is nothing but a periodically corrugated surface whose period is of the order of the visible wavelength. Incoming light experiences selective diffraction, a property at the very basis of any spectrophotometer. A compact disc acts as a diffraction grating under white light illumination because the digital information is engraved at the micron scale (Fig. 1a). Mankind was not the first to rule diffraction grating and Nature has used nanophotonic structures for a long time in the living world. Some butterfly wings showing nice iridescent colors are made of highly nanostructured materials that act as a diffraction grating having eventually photonic band gap properties (Biró et al. 2007) (Fig .1b).

Although the optical fields can be strongly modified far from a nanophotonic structure (Fig. 1), there has been recently a strong interest in investigating the structure of the light at its very vicinity (Novotny and Hecht 2006). The goal is to control the optical field at a scale, which is much smaller than the wavelength, opening new directions toward highly integrated nanophotonics devices for optical communication and nanoimaging. In the following, we will briefly discuss the two main assets of nanophotonic structures such as field localization and field enhancement.

Field localization

Because a nanophotonic structure is shaped at the nanometer scale, the electromagnetic field at its very vicinity exhibits subwavelength spatial variations. Figure 2a shows a closer look of the optical field at the surface of a compact disc recorded using near-field scanning optical microscopy (NSOM). The topography of Fig. 2a is clearly visible on the optical field. Using sharper nano-shaped structure leads to strong optical localization as illustrated in Fig. 2b, which shows the apex of an asymmetrical atomic force microscope (AFM) tip (left panel of Fig. 2 b) and its optical field under plane wave illumination (right panel of Fig. 2b). Because the tip radius of curvature is below 10 nm, the field is localized at this scale although the light wavelength is 633 nm.

Field enhancement

Another asset of nanophotonic structure is to provide a means to locally enhance the optical field. This property is

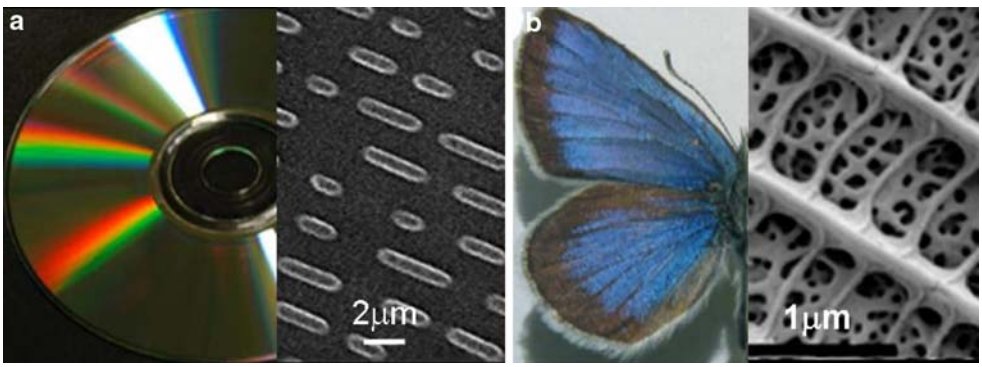

Fig. 1 Diffraction of light with nanophotonic structure. **a** A compact disc and a closer look of its surface. **b** Male butterfly *Albulina metallica* and a closer look of its dorsal wings (from (Biró et al. 2007))

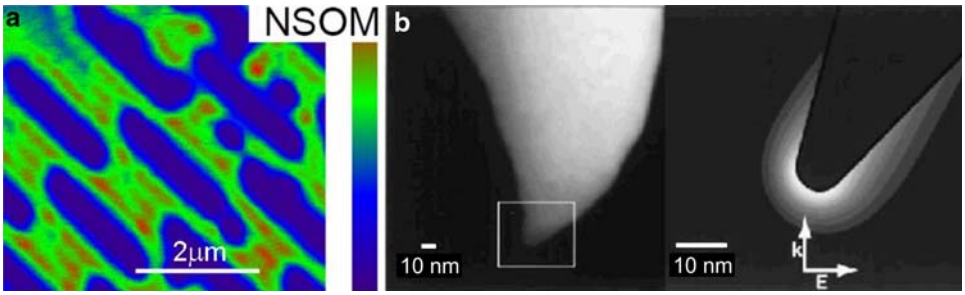

Fig. 2 Field localization with nanophotonic structures: **a** optical field at the surface of a compact disc (from Prof. Shalaev group, Purdue University). **b** Strongly localized optical field at metallized AFM tip (from Prof. S. Xie, Harvard University, Department of Chemistry and Chemical Biology)

linked to the spatial field confinement already discussed but also to local electromagnetic resonances that are especially strong in metallic nanostructures. These so-called 'plasmon resonances' are collective oscillations of electrons that exist for specific incoming optical frequencies. The electromagnetic mode associated with a plasmon resonance is called surface plasmon polariton (SPP) and can propagate at the metal dielectric interface. Figure 3a shows a nanophotonic structure made of silver and illuminated with a Gaussian laser beam at $\lambda = 573$ nm. A slit opens the structure and a pyramidal shape sits above the aperture. Figure 3b shows the field enhancement at the slit rim and at the pyramid apex. A field enhancement of 80 is possible thanks to the SPP (excited at the slit bottom) that propagates and concentrates at the pyramid apex.

Thanks to these unique properties, a nanophotonic structure can enhance and localize the optical field at nanometer scale. Furthermore, the field hot spot is usually at the metal interface in a position very attractive for optimal interaction with biomolecules in solution or attached to the surface. Alternatively, a nanostructure such as the slit of Fig. 3 defines a sub-wavelength observation volume that can be used for analysis of biomolecules as we will see in "Fluorescence correlation spectroscopy in nanoapertures: confined observation volumes".

Fluorescence correlation spectroscopy in nanoapertures: confined observation volumes

Molecules going in and out the observation volume yield fluctuations of the fluorescence intensity that can be quantified by fluorescence correlation spectroscopy (FCS), a method initially introduced by Webb and colleagues (Magde et al. 1972) (for reviews see Haustein and Schwille 2007; Webb 2001). FCS relies on the temporal analysis of the fluorescence intensity fluctuations, which we shortly describe in the following. When a single molecule diffuses across the observation volume, it emits fluorescence light during a time, which depends on the molecules' mobility and on the size of the observation volume (Fig. 4). Due to the stochastic movements of molecules, a large number of individual fluorescence bursts contribute to the collected intensity signal. Therefore, the physical parameters characterizing the molecules under study, such as their number and their mobility, are somehow hidden in the fluorescence intensity signal. By measuring the temporal correlation of the fluorescence intensity signal with itself [fluorescence autocorrelation function, (ACF), Fig. 4], FCS analysis recovers two main parameters: the average number of molecules N and their mean residence time in the observation volume τ_d. The autocorrelation is maximal at zero-time lag and equals $1/N$ for a perfect dye. It decreases within a characteristic time lag, which is usually defined at half maximum. For a free diffusion in two dimensions and a Gaussian excitation intensity of radius w (defined at $1/e^2$), the characteristic time equals τ_d and $\tau_d = w^2/(4D)$, where D is the diffusion coefficient. In addition to the number of molecules and the diffusion time, the shape of the autocorrelation function indicates the mode of diffusion (e.g., one-, two- or three-dimensional, free vs. anomalous diffusion).

Remarkably, FCS is able to provide a measure of the local concentration. Because FCS relies on the analysis of

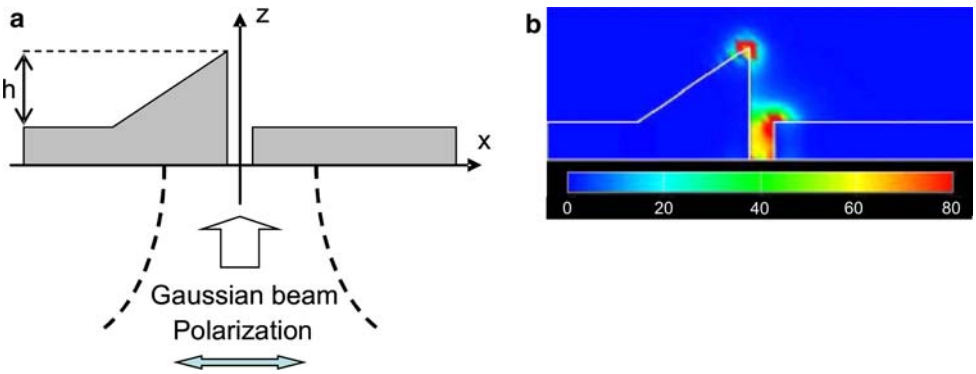

Fig. 3 Field enhancement in nanophotonic structures. **a** Structure: $\lambda = 573$ nm, $h = 109$ nm, film material: silver, film thickness 172 nm, slit width 36 nm. **b** The field enhancement at the pyramid apex reaches 80 (adapted from Tanaka et al. 2006)

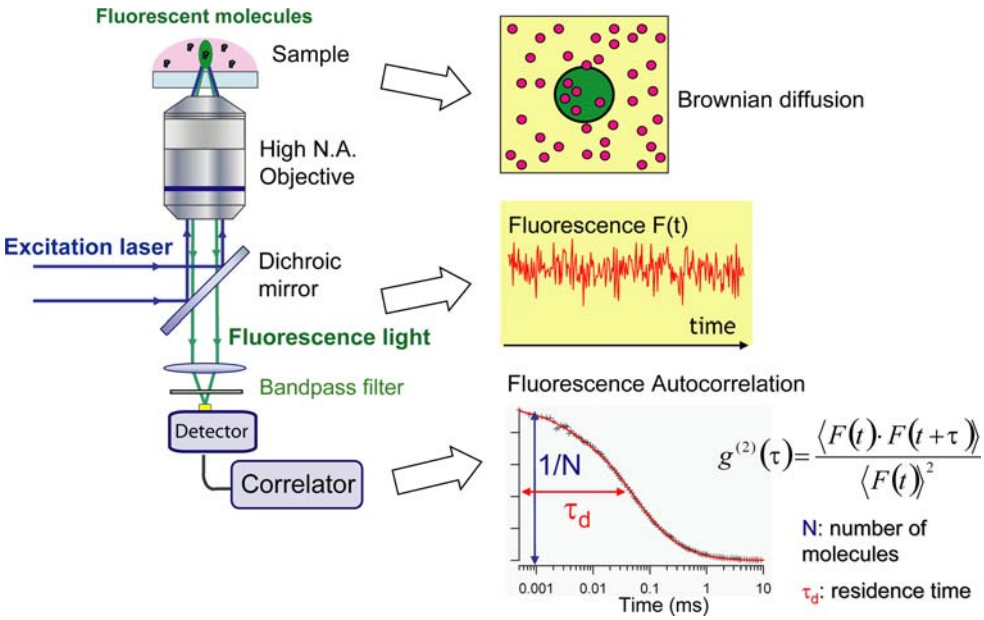

Fig. 4 Principles of fluorescence correlation spectroscopy. A tightly focused laser (*blue beam*) excites the fluorescence of molecules diffusing across the observation volume. The fluorescence light (*green beam*) is collected by a high-numerical aperture objective, spectrally filtered by a bandpass filter and detected onto a single-photon counting detector. The fluctuating fluorescence intensity is auto-correlated in order to determine two important characteristics, the number and the mean residence time of molecules in the observation volume

number fluctuations, it is particularly efficient for small N, typically ranging from 0.1 to 100 molecules, which corresponds to concentrations from 0.4 to 400 nM in a standard confocal volume (0.5 fL = 0.5 × 10^{-15} L = 0.5 μm^3).

To dramatically reduce the observation volume, the seminal work of Levene et al. (2003) suggested to perform FCS in nanoapertures (namely nanometer-size holes) milled in metal films (Fig. 5). Using such a scheme, the observation volume can be reduced by more than three orders of magnitude as compared to diffraction-limited spot. As a direct consequence, the range of accessible concentrations is extended to higher values (micromolar instead of nanomolar with diffraction-limited spots). This is particularly important for the study of enzyme kinetics at physiological concentrations (see "Biological applications"). By providing local measurements of diffusion properties at nanometric length-scale, observation volumes in nanoapertures allow also the study of the fine-grained cellular organizations, which are usually averaged over standard confocal volumes (see "Probing the mosaic nature of the plasma membrane").

Acting as a pinhole filter at the object plane, a single nanoaperture does not only reduce the observation volume but also facilitates optical alignments, especially in fluorescence cross-correlation spectroscopy (FCCS), which generally uses two excitation beams. FCCS consists in labeling hypothetical molecular partners with spectrally separable fluorophores and cross-correlating their fluorescence signals to get a measure of the association and colocalization efficiency (Bacia et al. 2006; Schwille et al. 1997). This powerful method requires the accurate overlapping of the two excitation beams and is generally difficult to implement. By confining the excitation beams in a defined observation volume and acting as a direct pinhole, the nanoapertures greatly simplifies these settings (Wenger et al. 2006a).

Fluorescence enhancement by a single aperture

A second striking, and quite unexpected effect, is the ability of nanoapertures to enhance the fluorescence emission. A nanometric aperture can affect the fluorescence emission in three ways: (1) by locally enhancing the excitation intensity, (2) by increasing the emitter's radiative rate and quantum efficiency, and (3) by modifying its radiation pattern, for a higher emission directionality toward the detectors. Determining the specific influence of these processes is a crucial issue to characterize nanodevices for enhanced fluorescence, and has been a topic of great interest for the last decade (Barnes 1998; Fort and Grésillon 2008, Lakowicz 2005). The inherent challenge in this task originates from the fact that the detected signal results from the product of excitation and emission processes. Excitation depends on the interaction between the driving field and the nanostructure, while at moderate optical intensities, the emission efficiency is set by the balance of radiative and non-radiative decays and the modification of the radiation pattern.

In 1986, Fischer suggested that fluorescence enhancement and reduced observation volumes could be obtained from random arrangements of small metal apertures (Fischer 1986). In 2003, single-molecule detection in an epifluorescence arrangement from a single subwavelength aperture was demonstrated in a high-concentration environment (Levene et al. 2003) (in which no fluorescence enhancement was reported). The fact that significant enhancement in excitation also occurs within a single nanoaperture was first demonstrated in a series of papers on single-molecule epifluorescence in round (Rigneault

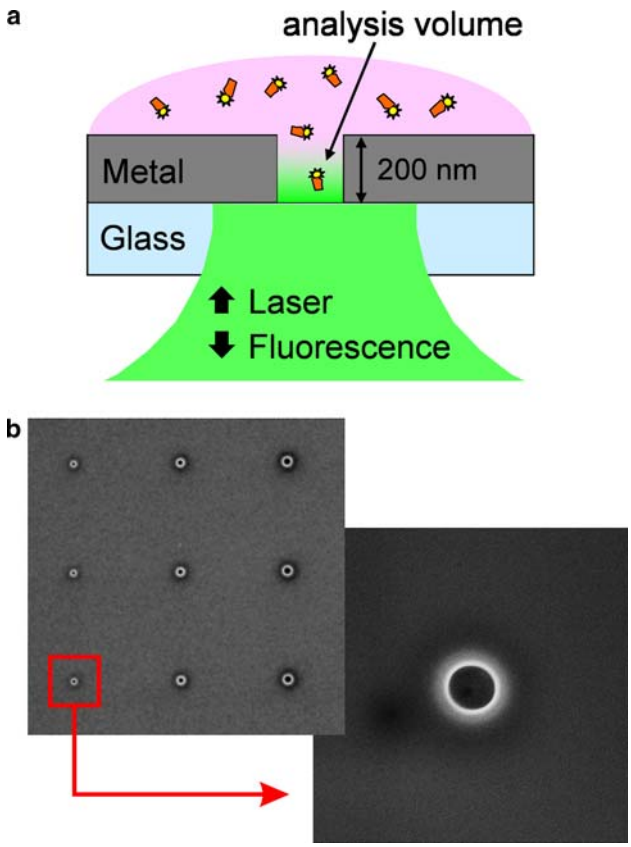

Fig. 5 **a** Arrangement for single nanoaperture-enhanced fluorescence. A fluorescent molecule located at the bottom of the aperture emits significantly more photons than the same molecule put in the diffraction-limited spot of a high-numerical aperture microscope objective. **b** SEM image of 150-, 220-, 360-nm diameter apertures milled by focused ion beam on a 200-nm thick aluminum film deposited over a standard glass coverslip, and close-up view of a 150-nm aperture (image courtesy of J. Dintinger, University Louis Pasteur, Strasbourg-France)

et al. 2005; Wenger et al. 2007a) and rectangular (Wenger et al. 2005) apertures. Using single rhodamine 6G molecules in isolated 150-nm diameter apertures milled in an aluminum film, a 6.5-fold enhancement of the fluorescence rate per molecule was reported as compared to free solution (Rigneault et al. 2005). This phenomenon was further investigated with a combination of FCS and fluorescence lifetime measurements to resolve the photokinetic rates of rhodamine 6G molecules in a water–glycerol mixture (Wenger et al. 2007a). The fluorescence lifetime appeared to be dramatically reduced inside the aperture, indicating that the molecular energy levels' branching ratios were strongly affected. For a properly tailored nanoaperture diameter of 150 nm, the aperture allowed for a higher radiative rate without decreasing the fluorophore quantum efficiency (fluorescence quenching). The combination of this effect together with an increase in the local excitation intensity led to the overall fluorescence enhancement. Excitation enhancement is further supported by computational models (Popov et al. 2006; Yuan et al. 2006; Shuford et al. 2007; Mahdavi et al. 2007). Additional studies demonstrated single-molecule detection under trans-illumination (Leutenegger et al. 2006), with comparatively lower enhancement levels, and in C-shaped apertures (Fore et al. 2007).

A metal supporting strong surface plasmon resonances in the visible range, such as gold, allows for even larger fluorescence enhancement factors. Two recent studies have focused on the case of Alexa Fluor 647 dye (quantum yield in water solution 30%) and nanoapertures milled in gold films (Gerard et al. 2008; Wenger et al. 2008). Nanometric apertures milled in gold exhibit significantly higher (50%) fluorescence enhancement factors than apertures in aluminum, with a maximum enhancement of 12 for a 120-nm diameter aperture in gold, as shown in Fig. 6. This effect is related to a larger enhancement of the excitation intensity and radiative rate. Due to the intrinsic permittivity of gold, the maximum enhancement for gold also occurs at a smaller aperture diameter, which is beneficial for single-molecule detection at high concentrations. Comparison with numerical simulations reveals that the fluorescence enhancement is maximal when the aperture diameter corresponds to a minimum of the group velocity of light inside the hole. This provides a guideline for the design of optimized nanostructures for enhanced fluorescence detection (Fig. 7).

Biological applications

Enhanced single-molecule analysis in solution

The common approach for single-molecule fluorescence analysis uses a confocal microscope with a high NA objective, which provides detection volumes of about 0.5 fL (= 0.5 μm^3). This limits the concentration for single-molecule analysis to a few nM. For artificial environments, this low concentration may not be a problem; however, it may be a crucial limitation for biological and biochemical studies, which typically involves concentrations in the µM to the mM range (Levene et al. 2003). Many enzymatic reactions are also naturally effective at ligand concentrations in this range. Arbitrarily reducing the ligand concentration may lead to chemical pathway alteration and artifacts. In this context nanophotonic structures provide a direct way to perform in vitro studies at more relevant concentrations.

As explained above, photonic structures can enhance the fluorescence emission and collection efficiencies by tailoring the molecules environment. This simultaneously increases the molecular brightness and reduces the detection volume, leading to a lower amount of background scattered light, and to a higher concentration available for

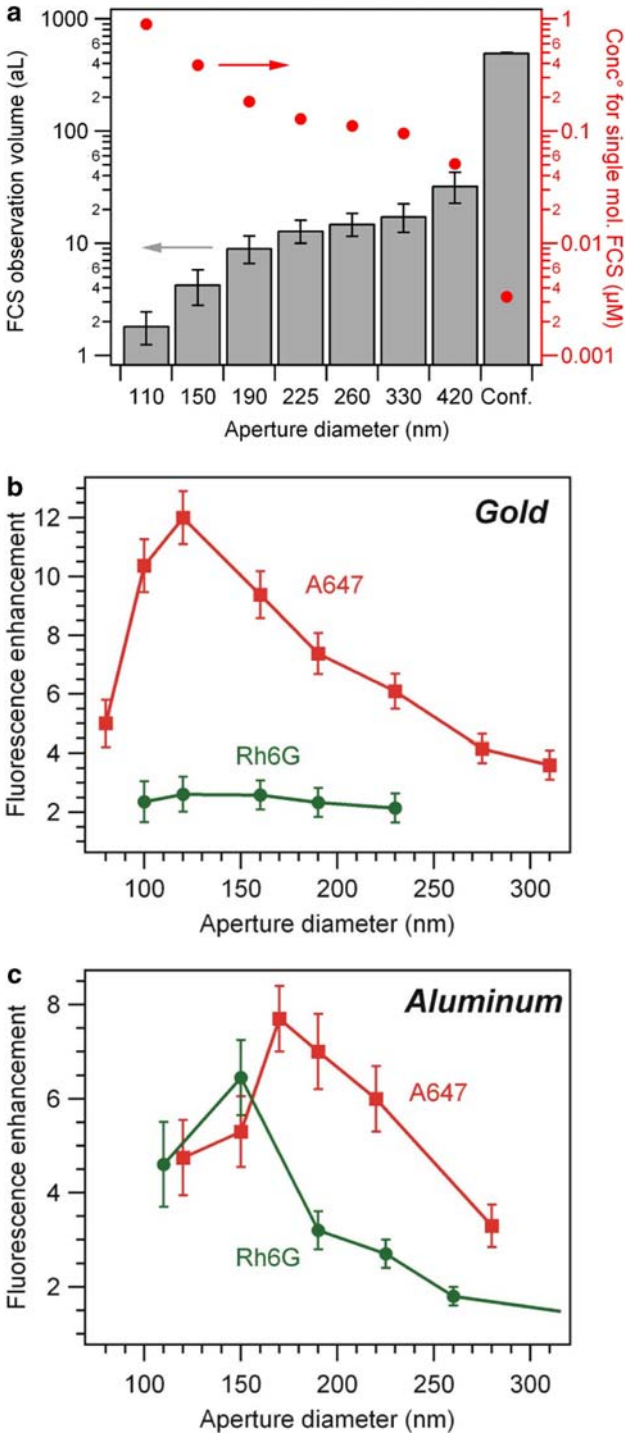

◀ **Fig. 6** FCS in metallic nanoapertures. **a** Observation volumes in attoliter (10^{-18} L) measured by FCS for nanoapertures milled in aluminum (rhodamine 6G dyes, 488 nm excitation) and the corresponding concentration to ensure an average number of one molecule in the observation volume (*right scale*). Experimental single-molecule fluorescence enhancement versus aperture diameter, for apertures milled in gold (**b**) and aluminum (**c**) films. Rhodamine 6G (Rh6G) dyes were excited at 488 nm, and their fluorescence was collected in the 510–560 nm range. Alexa Fluor 647 (A647) dyes were excited at 633 nm, and their fluorescence was collected in the 650–690 nm range. These curves show significant differences between apertures milled in gold or in aluminum, and highlight the need for a layer exhibiting a strong metallic character at the excitation wavelength to obtain enhanced fluorescence

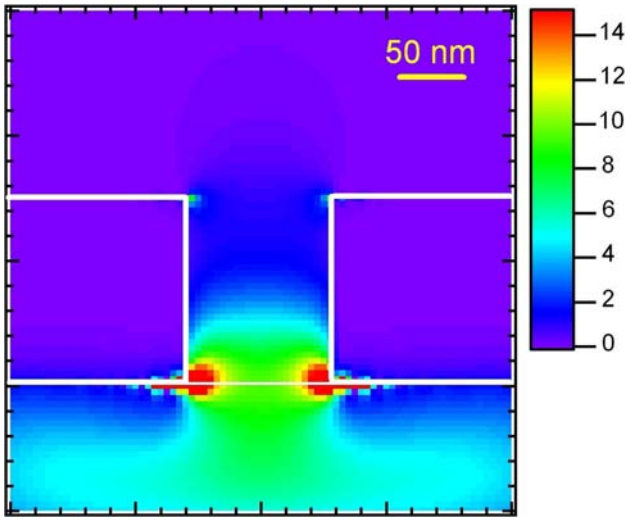

Fig. 7 Three-dimensional finite-element time-domain simulation of the intensity distribution (*linear scale*) for a nanoaperture milled in gold with 120-nm diameter and 150-nm thickness. The substrate was taken to glass, while the upper medium and the aperture inside were taken to pure water. The illumination was set to uniform intensity distribution (*plane wave*) with free space wavelength of 633 nm, and linear polarization parallel to the plane viewed here

single-molecule studies, as shown in Fig. 6a. Several methods allowing a simultaneous decrease of the detection volume and increase of the fluorescence signal have been proposed so far, and are reviewed in (Blom et al. 2006).

In spite of their conceptual simplicity, nanoapertures possess appealing properties to increase the effectiveness of fluorescence-based single-molecule detection, such as localization of excitation light, strong isolation from emission produced by unbound species, and an increase in apparent absorption and emission yield (Craighead 2006; Genet and Ebbesen 2007; Mannion and Craighead 2007). The significant fluorescence increase obtained for small radius apertures appears especially interesting because it allows for the possibility to significantly reduce the observation volume while still detecting a sufficient signal. This yields an efficient signal-to-background discrimination, even with attoliter (10^{-18} L) volumes and single-molecule resolution. Using nanoapertures, a large range of biological processes have been efficiently monitored with single-molecule resolution at micromolar concentrations (Leutenegger et al. 2006; Levene et al. 2003; Samiee et al. 2005; Wenger et al. 2006a). For instance, FCS with nanoapertures was used to study the oligomerization of the bacteriophage λ repressor protein at micromolar concentrations (Samiee et al. 2005). This approach confirmed the previous results on binding constants but also provided new insights on diffusion changes resulting from binding events.

Moreover, the studies on nanoaperture-enhanced fluorescence point out that for a properly tailored aperture, count rates per molecule greater than a few hundred thousands photons per second were readily obtained, whereas for a single molecule in open solution, fluorescence saturation prevents the count rate from exceeding a few tens of thousands counts per second. Interestingly the signal-to-noise ratio in FCS increases as the square of the fluorescence count rate per molecule (for a complete discussion see Zander et al. 2002). Consequently, a count rate enhancement per molecule by a factor of 10 allows a 100-fold reduction in experiment duration while retaining the same signal-to-noise ratio. This may offer new possibilities for fast and reliable screening for single molecules.

Real-time single-molecule DNA sequencing

Performing high-throughput, high-accuracy DNA sequencing at low costs has become a major issue, largely attracted by the growing potential of quantitative genomics. For this cutting edge application, nanometric apertures offer specific advantages as they enable the observation of single fluorophores against a dense background by maintaining a high signal-to-noise ratio. Moreover, nanoapertures can be operated in massive parallelism, allowing for high-speed DNA analysis.

This concept has been developed since 2004 by Pacific Biosciences, a private company formed by researchers at Cornell University. Each nanoaperture forms a nano-observation chamber for watching DNA polymerase as it performs sequencing by synthesis (Fig. 8). Within each chamber, a single DNA polymerase molecule is attached to the bottom surface so that it persists in the detection volume. Fluorescently labeled nucleotides diffuse into the reaction solution at high concentrations to promote enzyme speed and accuracy. When the DNA polymerase encounters the nucleotide complementary to the next base in the template, it is incorporated into the duplicated DNA chain. During the incorporation process, the enzyme holds the nucleotide in the detection volume for a few tens of milliseconds, much longer than the average residence time of the diffusing nucleotides. This causes a millisecond fluorescence flash to occur, which is detected with a CCD camera. As each nucleotide (A, T, G, C) bears a different color marker, the spectral analysis of the fluorescence flash allows to discriminate the incorporated nucleotide, which constructs the DNA sequence step by step. Then, as part of the natural incorporation cycle, the polymerase cleaves the bond holding the fluorophore in place and the dye diffuses out of the detection volume. This ensures that the duplicated DNA strand is purely natural, i.e., it does not bear any fluorescent material. Following incorporation, the signal quickly returns to the baseline. Then, the polymerase advances to the next base and the process continues to repeat, adding nucleotides one by one.

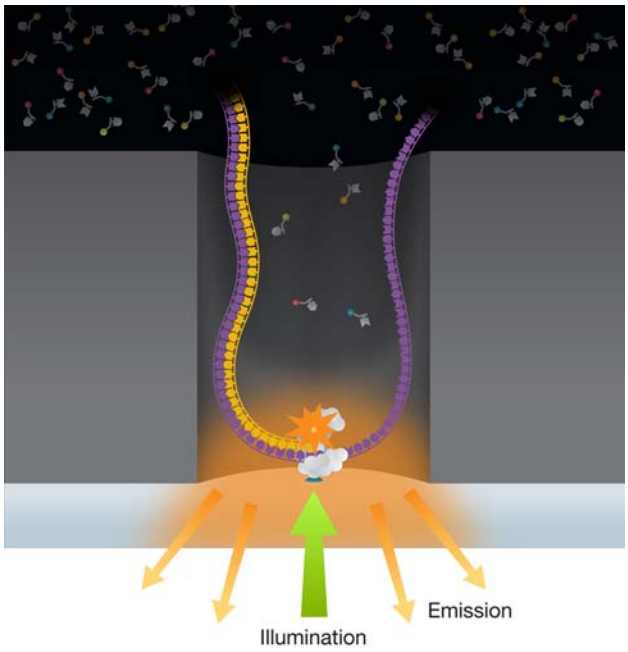

Fig. 8 Single nanometric aperture for real-time single-molecule DNA sequencing. A DNA polymerase molecule attached to the bottom surface is used to successively incorporate fluorescent nucleotides complementary to the DNA strand, causing fluorescence bursts for each incorporation process (see text for details). Image copyright of Pacific Biosciences Inc., reprinted with permission

DNA sequencing is observed as it occurs in real-time across thousands of nanoapertures that can be operated simultaneously. Acting uninterrupted, the DNA polymerase keeps on incorporating bases at a speed of ten per second. Researchers at Pacific Biosciences demonstrated that DNA strands of thousands of nucleotides in length could be accurately sequenced. This sequencing has a wide range of applications, yet many technological issues have to be addressed. These mostly deal with polymerase enzymatic activity and large scale nanoaperture detection. Selective aluminum passivation for targeted immobilization of single DNA polymerase molecules in nanoapertures is described in Korlach et al. (2008). Improved manufacturing techniques of nanoapertures on a large-scale wafer are described in Foquet et al. (2008), while progress toward large scale detection of thousands of nanoapertures in parallel are presented in Lundquist et al. (2008).

Probing the mosaic nature of the plasma membrane

The significance of cell membrane organization has become broadly appreciated since micrometer-scale domains were experimentally identified in the plasma membrane of living fibroblasts (Yechiel and Edidin 1987).

The concept has been refined with the identification of both lipid-dependent and cytoskeleton-based organizations as the main compartmentalizing forces at work at the plasma membrane (Edidin 2003; Kusumi et al. 2005; Marguet et al. 2006; Simons and Ikonen 1997).

Such understanding has greatly benefited from advanced biophotonic techniques. Among them, fluorescence correlation spectroscopy (FCS) which can be performed at physiological temperature on living cells, has successfully contributed unraveling lateral membrane heterogeneities (Haustein and Schwille 2007; Marguet et al. 2006). This is because FCS averages thousands of single-diffusion events at a very low level of probe concentration, a critical requirement in membrane organization studies. Another great advantage of the FCS is the possibility to accurately quantify local measurements of molecular mobility on different temporal scales. Among the different nanotechnologies applied on biomembranes (Torres et al. 2008), the ones combining single nanometric aperture technology with FCS have great potential as recently demonstrated (Edel et al. 2005; Moran-Mirabal et al. 2007; Samiee et al. 2006; Wenger et al. 2006b). Indeed, these approaches preserve the FCS temporal resolution while providing a sub-wavelength spatial resolution. As explained above, nanoholes can act as pinholes directly located under the cell membrane. These allow narrowing the observation area below the diffraction limit (Fig. 9).

The nanoholes used so far for membrane studies are circular apertures with radii between 50 and 250 nm milled in an opaque aluminum film covering a glass coverslip. On the top of which, adherent cells keep their capability to attach and expand without particular difficulty (Edel et al. 2005; Wenger et al. 2007b). Moreover, electron microscopy observations have clearly demonstrated that cells explored the surface they are attached to and, due to active polymerization of acti filaments, formed filopodia-like extensions entering the nanoapertures (Moran-Mirabal et al. 2007).

It is therefore possible to perform FCS measurements to study the diffusion of fluorescent probes on plasma membrane surfaces smaller than the smallest ones usually probed by classical fluorescence microscopy. Diffusion measurements by FCS in nanoapertures have been reported for lipid analogs incorporated in rat basophilic cell membranes. Indeed, DiIC12 showed faster lateral diffusion than the C16 DiI analog (Moran-Mirabal et al. 2007). These observations were consistent with the differential properties of lipid packing and lipid–lipid interactions.

However, when performed at a single size collection volume, the measurements established by FRAP or FCS provide little information on the mode of diffusion. As emphasized in the seminal work of Yechiel and Edidin (1987) in the context of FRAP, diffusion measurements in confocal volumes can be performed at different observation

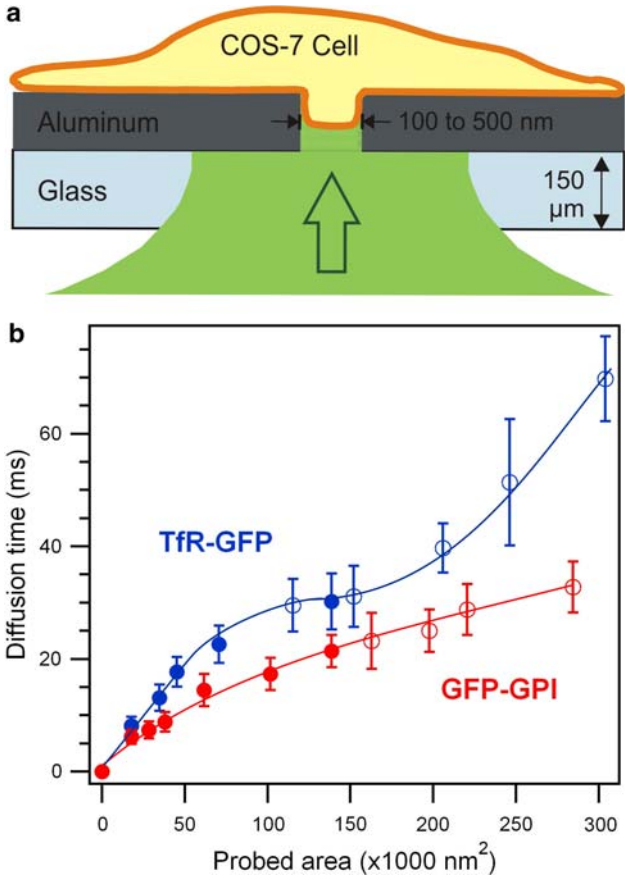

Fig. 9 **a** Single nanoaperture to probe a sub-diffraction area on a live cell plasma membrane. **b** Average diffusion time probed by FCS versus the aperture area for two types of chimeric proteins embedded in the cell plasma membrane. *Open markers* correspond to open beam measurements, *solid markers* refer to the nanoaperture experiments. *Lines* are guides to the eyes

volumes to overcome this limitation. By plotting the apparent τ_d of a membrane component against the square of the transversal waist (radius) of the confocal spot, it is possible to establish the so-called "FCS diffusion law" (Lenne et al. 2006; Wawrezinieck et al. 2005). In a free diffusive system, a strict linear relationship does exist between these two parameters. However, any deviation from the origin of the intercept on the time axis will be the signature of a possible confinement.

In a first set of experiments, the area of measured membrane was modified by using laser beams of different size but limited by the optical resolution of the microscope (Lenne et al. 2006). Therefore, the diffusion mode was deduced by extrapolating the straight lines on the time axis. Computer simulations were carried out to provide hints for understanding these experimental observations (Wawrezinieck et al. 2005). The principle of these simulations was to decipher the theoretical ACF and consequently the diffusion laws of molecules whose diffusion was hindered either by a meshwork or isolated domains. Interestingly, the time

axis intercept t_0 appeared to be a key parameter when determining the type of confinement; t_0 being positive for diffusion in isolated microdomains, negative for corrals, and null for free diffusion. Strikingly, our experiments showed that the diffusion law of the transferrin receptor TfR-GFP (known to interact with the cytoskeleton) had a negative t_0 value, whereas that of the raft marker fluorescent ganglioside GM1 (FL-GM1) exhibited a positive t_0 value. It is important to mention that the t_0 value indicates a type of confinement in terms of physical boundaries (impermeable obstacles, dynamic partitioning into discrete domains or free diffusion restricted by corrals), but not the biochemical nature of these impediments. This should be identified by appropriate pharmacologic treatments to further characterize the origin of the confinement (see Lasserre et al. 2008; Lenne et al. 2006).

Nonetheless, one could argue that t_0 values arise from the extrapolation of the diffusion laws for non-optically accessible values, and that we can only speculate on what would experimentally happen in such circumstances, especially since microdomains are thought to be far much smaller (Edidin 2003; Kusumi et al. 2005; Marguet et al. 2006; Simons and Ikonen 1997).

To overcome this issue, the use of nanometric apertures extends the initial experimental FCS approach (Wenger et al. 2007b). Cos-7 cells were seeded on these coverslips, and FCS diffusion times were measured on the basal plasma membrane of the cells extending in the nanoholes.

Except the freely diffusing fluorescent analog of phosphatidylcholine FL-PC, decreasing the diameter of surface of observation led to transient diffusion regimes. Based upon the experimental results and simulations, it has been possible to demonstrate that changes in the shapes of the diffusion curves were purely dependent on the geometrical dimensions of heterogeneity of the plasma membrane, thus enabling the precise specification of the average size of membrane rafts.

For FL-GM1, two distinct diffusion regimes were revealed, dependent on the aperture radii. Below a characteristic radius value of 100 nm, the diffusion time increased rapidly and linearly as a function of nanohole radius, intercepting the origin. Beyond 100 nm, diffusion time progression slowed dramatically to an affine function with a positive t_0 (16.3 ± 1.5 ms), merging nicely with the diffusion law obtained at diffusion limited spots. Similar inflection between the two diffusion regimes was observed when studying GFP-GPI (transition radius around 120 nm). Cholesterol oxydase treatment led to a free-like linear diffusion, comparable to that obtained with FL-PC. Microdomain model simulations allowed the estimation of a ratio of 10 for the occurrence of the transition between the probed area and the domain area. We thereby calculated the radius of the GM1 and GFP-GPI containing microdomains as respectively 40 and 30 nm.

Analysis of the diffusion of TfR-GFP was carried out in the same way. According to the consensus view, TfR displays mainly cytoskeleton-based confinement (Fujiwara et al. 2002). However, the t_0 value after treatment with high doses of cytochalasin D (10 μM) reverted to a positive value (7.8 ± 1.6 ms), which could be abrogated by concomitant treatment with cholesterol oxydase (0.2 ± 0.1 ms) (Lenne et al. 2006). Interpretation of these results was that the two types of confinement co-exist to affect TfR diffusion. Nanoapertures have provided experimental validation of this hypothesis, since two transition regimes were found: one around 50 nm (radius of domains) and a second around 230 nm (size of the cytoskeletal meshes).

Therefore, these approaches not only permit the analysis of the nature and strength of confinements, but also supply pertinent and reliable information on the geometrical dimensions of the domains and/or meshwork governing the diffusion for each type of molecules. Altogether, this experimental approach provides a robust frame to investigate lateral heterogeneities in cellular membranes. By measuring the transit times of a given molecule at different spot sizes with FCS, different modes of lateral diffusion can be probed as illustrated in Fig. 9. We have characterized so far three modes of diffusion: (1) free/free-like diffusion; (2) confined diffusion mediated by dynamic partitioning into discrete microdomains surrounded by membrane regions of different properties, or by transient molecular assembly; and (3) confined diffusion, mediated by the build up of a meshwork with assembled domains of similar properties, intersected by barriers (Lenne et al. 2006; Wawrezinieck et al. 2005).

Conclusion

Milling nanometric apertures in a metallic film is an intuitive way to manufacture new nanophotonics devices that are robust and highly reproducible. Although the concept appears very simple, such apertures exhibit attractive properties for biophotonics, such as localization of excitation light, strong isolation from emission produced by species located outside the aperture, and an increase in the fluorescence signal. The simplicity of the structures and their ease of use should further expand their application towards the real-time detection and identification of a low number of molecules.

Methods for the preparation of cost-effective organized patterns of metallic nanoapertures on a large scale are now available. Focused ion beam milling, electron beam lithography and photolithography can be employed. As an alternative, laser-induced optical breakdown by femtosecond pulses can be envisioned, thanks to a sharp threshold for

laser-induced material damage. This should allow for a wide range of applications in biophotonics, enabling significant research and even commercial applications.

We expect that nanophotonic structures such as metallic nanoapertures will provide new avenues to study complex materials such as living cells. They will help to probe and to characterize dynamic events occurring at the nanometric scale and will shed light on signaling processes in nanodomains/molecular complexes in the plasma membrane or its vicinity.

Acknowledgments The authors acknowledge the stimulating discussions with S. Blair, N. Bonod, T. W. Ebbesen, D. Gérard and E. Popov. This work was supported by institutional grants from Institut National de la Santé et de la Recherche Médicale (INSERM) and Centre National de la Recherche Scientifique (CNRS) and by specific grants from Agence Nationale de la Recherche (ANR), Association pour la Recherche sur le Cancer (ARC), The National Cancer Institute (INCa), and CNRS.

References

Barnes WL (1998) Fluorescence near interfaces: the role of photonic mode density. J Mod Opt 661–699

Bacia K, Kim SA, Schwille P (2006) Fluorescence cross-correlation spectroscopy in living cells. Nat Methods 3:83–89

Betzig E, Patterson GH, Sougrat R, Lindwasser OW, Olenych S, Bonifacino JS, Davidson MW, Lippincott-Schwartz J, Hess HF (2006) Imaging intracellular fluorescent proteins at nanometer resolution. Science 313:1642–1645

Biró LP, Kertész K, Vértesy Z, Márk GI, Bálint Z, Lousse V, Vigneron J-P (2007) Living photonic crystals: butterfly scales—nanostructure and optical properties. Mater Sci Eng 27:941–946

Blom H, Kastrup L, Eggeling C (2006) Fluorescence fluctuation spectroscopy in reduced detection volumes. Curr Pharm Biotechnol 7:51–66

Craighead HG (2006) Future lab-on-a-chip technologies for interrogating individual molecules. Nature 442:387–393

Edel JB, Wu M, Baird B, Craighead HG (2005) High spatial resolution observation of single molecule dynamics in living cell membranes. Biophys J 88:L43–L45

Edidin M (2003) Lipids on the frontier: a century of cell-membrane bilayers. Nat Rev Mol Cell Biol 4:414–418

Fischer UC (1986) Submicrometer aperture in a thin metal film as a probe of its microenvironment through enhanced light scattering and fluorescence. J Opt Soc Am B 3:1239–1244

Foquet M, Samiee KT, Kong X, Chaudhuri BP, Lundquist PM, Turner SW, Freudenthal J, Roitman DB (2008) Improved fabrication of zero-mode waveguides for single-molecule detection. J Appl Phys 103:034301

Fore S, Yuen Y, Hesselink L, Huser T (2007) Pulsed-interleaved excitation FRET measurements on single duplex DNA molecules inside C-shaped nanoapertures. Nano Lett 7:1749–1756

Fort E, Grésillon S (2008) Surface enhanced fluorescence. J Phys D Appl Phys 41:013001

Fujiwara T, Ritchie K, Murakoshi H, Jacobson K, Kusumi A (2002) Phospholipids undergo hop diffusion in compartmentalized cell membrane. J Cell Biol 157:1071–1081

Genet C, Ebbesen TW (2007) Light in tiny holes. Nature 445:39–46

Gerard D, Wenger J, Bonod N, Popov E, Rigneault H, Mahdavi F, Blair S, Dintinger J, Ebbesen T (2008) Nanoaperture-enhanced fluorescence: towards higher detection rates with plasmonic metals. Phys Rev B 77:045413

Haustein E, Schwille P (2007) Fluorescence correlation spectroscopy: novel variations of an established technique. Annu Rev Biophys Biomol Struct 36:151–169

Klar TA, Hell SW (1999) Subdiffraction resolution in far-field fluorescence microscopy. Opt Lett 24:954–956

Korlach J, Marks PJ, Cicero RL, Gray JJ, Murphy DL, Roitman DB, Pham TT, Otto GA, Foquet M, Turner SW (2008) Selective aluminum passivation for targeted immobilization of single DNA polymerase molecules in zero-mode waveguide nanostructures. Proc Natl Acad Sci USA 105:1176–1181

Kusumi A, Nakada C, Ritchie K, Murase K, Suzuki K, Murakoshi H, Kasai RS, Kondo J, Fujiwara T (2005) Paradigm shift of the plasma membrane concept from the two-dimensional continuum fluid to the partitioned fluid: high-speed single-molecule tracking of membrane molecules. Annu Rev Biophys Biomol Struct 34:351–378

Lakowicz JR (2005) Radiative decay engineering 5: metal-enhanced fluorescence and plasmon emission. Anal Biochem 337:171–194

Lasserre R, Guo XJ, Conchonaud F, Hamon Y, Hawchar O, Bernard AM, Soudja SM, Lenne PF, Rigneault H, Olive D et al (2008) Raft nanodomains contribute to Akt/PKB plasma membrane recruitment and activation. Nat Chem Biol 4:538–547

Lenne PF, Wawrezinieck L, Conchonaud F, Wurtz O, Boned A, Guo XJ, Rigneault H, He HT, Marguet D (2006) Dynamic molecular confinement in the plasma membrane by microdomains and the cytoskeleton meshwork. EMBO J 25:3245–3256

Leutenegger M, Gösch M, Perentes A, Hoffmann P, Martin OJF, Lasser T (2006) Confining the sampling volume for fluorescence correlation spectroscopy using a subwavelength sized aperture. Opt Express 14:956–969

Levene MJ, Korlach J, Turner SW, Foquet M, Craighead HG, Webb WW (2003) Zero-mode waveguides for single-molecule analysis at high concentrations. Science 299:682–686

Lundquist PM, Zhong CF, Zhao P, Tomaney AB, Peluso PS, Dixon J, Bettman B, Lacroix Y, Kwo DP, McCullough E et al (2008) Parallel confocal detection of single molecules in real time. Opt Lett 33:1026–1028

Magde D, Elson EL, Webb WW (1972) Thermodynamic fluctuations in a reacting system—measurement by fluorescence correlation spectroscopy. Phys Rev Lett 29:705

Mahdavi F, Liu Y, Blair S (2007) Modeling fluorescence enhancement from metallic nanocavities. Plasmonics 2:129–142

Mannion JT, Craighead HG (2007) Nanofluidic structures for single biomolecule fluorescent detection. Biopolymers 85:131–143

Marguet D, Lenne PF, Rigneault H, He HT (2006) Dynamics in the plasma membrane: how to combine fluidity and order. EMBO J 25:3446–3457

Moran-Mirabal JM, Torres AJ, Samiee KT, Baird B, Craighead HG (2007) Cell investigation of nanostructures: zero-mode waveguides for plasma membrane studies with single molecule resolution. Nanotechnology 18:195101

Novotny L, Hecht B (2006) Principles of nano-optics. Cambridge University Press, Cambridge

Popov E, Nevière M, Wenger J, Lenne P-F, Rigneault H, Chaumet P, Bonod N, Dintinger J, Ebbesen TW (2006) Field enhancement in single subwavelength apertures. J Opt Soc Am A 23:2342–2348

Rigneault H, Capoulade J, Dintinger J, Wenger J, Bonod N, Popov E, Ebbesen TW, Lenne PF (2005) Enhancement of single-molecule fluorescence detection in subwavelength apertures. Phys Rev Lett 95:117401–117404

Rust MJ, Bates M, Zhuang X (2006) Sub-diffraction-limit imaging by stochastic optical reconstruction microscopy (STORM). Nat Methods 3:793–795

Samiee KT, Foquet M, Guo L, Cox EC, Craighead HG (2005) lambda-Repressor oligomerization kinetics at high concentrations using

fluorescence correlation spectroscopy in zero-mode waveguides. Biophys J 88:2145–2153

Samiee KT, Moran-Mirabal JM, Cheung YK, Craighead HG (2006) Zero mode waveguides for single-molecule spectroscopy on lipid membranes. Biophys J 90:3288–3299

Schwille P, Meyer-Almes F-J, Rigler R (1997) Dual-color fluorescence cross-correlation spectroscopy for multicomponent diffusional analysis in solution. Biophys J 72:1878–1886

Schmidt R, Wurm CA, Jakobs S, Engelhardt J, Egner A, Hell SW (2008) Spherical nanosized focal spot unravels the interior of cells. Nat Methods 5:539–544

Shuford KL, Ratner MA, Gray SK, Schatz GC (2007) Electric field enhancement and light transmission in cylindrical nanoholes. J Comput Theor Nanosci 4:239–246

Simons K, Ikonen E (1997) Functional rafts in cell membranes. Nature 387:569–572

Tanaka K, Tanaka M, Sugiyama T (2006) Creation of strongly localized and strongly enhanced optical near-field on metallic probe-tip with surface plasmon polariton. Opt Express 14:832–846

Torres AJ, Wu M, Holowka D, Baird B (2008) Nanobiotechnology and cell biology: micro and nanofabricated surfaces to investigate receptor-mediated signaling. Annu Rev Biophys 37:265–288

Wawrezinieck L, Rigneault H, Marguet D, Lenne PF (2005) Fluorescence correlation spectroscopy diffusion laws to probe the submicron cell membrane organization. Biophys J 89:4029–4042

Webb WW (2001) Fluorescence correlation spectroscopy: inception, biophysical experimentations, and prospectus. Appl Opt 40:3969–3983

Wenger J, Lenne P, Popov E, Rigneault H, Dintinger J, Ebbesen T (2005) Single molecule fluorescence in rectangular nano-apertures. Opt Express 13:7035–7044

Wenger J, Gerard D, Lenne P, Rigneault H, Dintinger J, Ebbesen T, Boned A, Conchonaud F, Marguet D (2006a) Dual-color fluorescence cross-correlation spectroscopy in a single nanoaperture: towards rapid multicomponent screening at high concentrations. Opt Exp 14:12206–12216

Wenger J, Rigneault H, Dintinger J, Marguet D, Lenne P (2006b) Single-fluorophore diffusion in a lipid membrane over a subwavelength aperture. J Biol Phys 32:SN1–SN4

Wenger J, Cluzel B, Dintinger J, Bonod N, Fehrembach A, Popov E, Lenne P, Ebbesen T, Rigneault H (2007a) Radiative and nonradiative photokinetics alteration inside a single metallic nanometric aperture. J Chem Phys C 111:11469–11474

Wenger J, Conchonaud F, Dintinger J, Wawrezinieck L, Ebbesen TW, Rigneault H, Marguet D, Lenne PF (2007b) Diffusion analysis within single nanometric apertures reveals the ultrafine cell membrane organization. Biophys J 92:913–919

Wenger J, Gerard D, Dintinger J, Mahboub O, Bonod N, Popov E, Ebbesen TW, Rigneault H (2008) Emission and excitation contributions to enhanced single molecule fluorescence by gold nanometric apertures. Opt Express 16:3008–3020

Yechiel E, Edidin M (1987) Micrometer-scale domains in fibroblast plasma membranes. J Cell Biol 105:755–760

Yuan HX, Xu BX, Wang HF, Chong TC (2006) Field enhancement of nano-sized metal aperture with and without surrounding corrugations through resonant surface plasmons. Jpn J Appl Phys 45:787–791

Zander C, Keller R, Enderlein J (2002) Single molecule detection in solution: methods and applications. Wiley, New York